Non-classical Energy Conservation in Multi-wave Systems: "*Extra Energy*", "*Negative Energy*" and "*Annihilation of Energy*"

S.V. Kukhlevsky
Department of Physics, University of Pécs, Ifjúság u. 6, H-7624 Pécs, Hungary

The energy conservation is a general law of nature. In the classical physics, the energy W_{AB} of a conservative system AB that contains the objects A and B is equal to a sum of the positive energies W_A and W_B of the isolated objects A and B, $W_{AB} = W_A + W_B$. We show that the energy conservation does not exhibit the "classic law" ($W_{AB} \neq W_A + W_B$) if the physical objects are waves or they do have a wave nature of microscopic (quantum) objects. The "*extra energy*", "*negative* energy" and "*annihilation of energy*" are predicted for multi-wave (multi-beam) systems. The paradoxical phenomenon is demonstrated in context of the extraordinary transmission of light and matter through subwavelength aperture arrays assisted by surface waves [T.W. Ebbesen et al., Nature (London) 391, 667 (1998)) and E. Moreno et al., Phys. Rev. Lett. 95, 170406 (2005)]. The physical mechanism of "non-classic energy conservation" provides the transmission enhancement ("*extra energy*") not by coupling to the surface waves but by interference between diffracted waves (beams) in the far field. Furthermore, the "*annihilation of energy*" by destructive interference of fields at the detector leads to the zero transmission. Another surprising prediction of the model is a weak Wood's anomaly, which is present in a classical Young type two-slit system. The Wood anomalies in transmission spectra of optical gratings, a long standing problem in optics, follows naturally from interference properties of the model. We believe that the "non-classic energy conservation" demonstrated in the present paper gains physical inside into the nature of energy conservation. The physical mechanism of the "*extra energy*", "*negative* energy" and "*annihilation of energy*" affects the energy conservation in all subwavelength systems, for an example, in nanooptics and nanophotonics based on transmission and beaming of light or matter by subwavelengths apertures.

PACS numbers: 42.25.Bs, 42.25.Fx, 42.79.Ag, 42.79.Dj

The scattering of waves by apertures is one of the basic phenomena in the wave physics. The most remarkable feature of the light scattering by subwavelength apertures in a metal screen is enhancement of the light by excitation of electron waves in the metal. Since the observation of enhanced transmission of light through a 2D array of subwavelength metal nanoholes [1], the phenomenon attracts increasing interest of researchers because of its potential for applications in nanooptics and nanophotonics [2]. Recently, the enhanced transmission through subwavelength apertures was predicted also for matter waves [3]. The enhancement of light is a process that can include resonant excitation and interference of surface plasmons [3, 4, 5, 6], Fabry-Perot-like intraslit modes [7, 8, 9, 10], and evanescent electromagnetic waves at the metal surface [11]. In the case of thin screens whose thickness are too small to support the intraslit resonance, the extraordinary transmission is caused by the excitation of surface plasmons or their matter-wave analog, surface matter waves [3, 4, 5, 6]. In this Letter, we show another mechanism that provides a great transmission enhancement not by coupling to the surface electron or matter waves but by interference of diffracted waves in the far field.

The transmission enhancement without assistant of surface waves can be explained in terms of the following theoretical formulation. We first consider the transmission of light through a structure that is similar but simpler than an array of holes, namely an array of parallel subwavelength slits. The structure consists of a thin metal screen with the slits separated by many wavelength. To exclude the plasmons from our model, the metal is considered to be a perfect conductor. Such a metal is described by the classic Drude model for which the plasmon frequency tends towards infinity. Owing to the great distance between the slits, the electromagnetic field at one slit is assumed to be independent from other slits. The transmission of the slit array is determined by calculating the light power in the far-field diffraction zone. The waves diffracted by each of the independent slits are found by using the Neerhoff and Mur approach, which uses a Green's function formalism for a rigorous numerical solution of Maxwell's equations for a single, isolated slit [12, 13, 14]. The calculations show a big, up to 5 times, resonant transmission enhancement near to the Fabry-Perot wavelengths determined by an array period. To clarify the numerical result, we then present an intuitively transparent analytical model, which quantitatively explains the resonant enhancement in terms of the far-field interference of the propagating waves produced by the independent slits. The model predicts the $\sim$5-times (resonant) and $\sim$1000-times (nonresonant) enhancements for both the light and matter waves passing through a perforated metallic or dielectric screen, independently on the apertures shape. Verification of the analytical formulae by comparison with data published in the literature supports these predictions. The Wood anomalies in transmission spectra of optical gratings, a

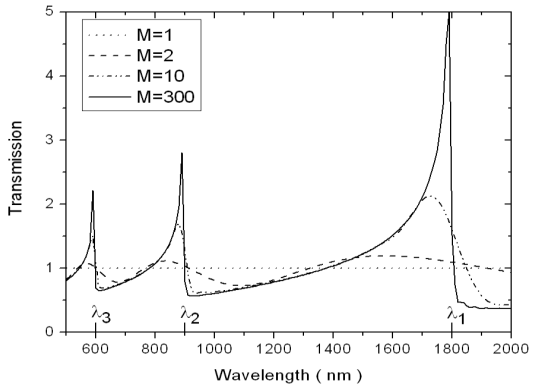

FIG. 1: The per-slit transmission $T_M(\lambda)$ of an array of independent slits of the period Λ versus the wavelength for different number M of slits. There are three Fabry-Perot like resonances at the wavelenghts $\lambda_n \approx \Lambda/n$, n=1, 2 and 3.

long standing problem in optics [15], follow naturally from interference properties of the model.

Let us first investigate the light transmission by using the rigorous model. The model considers an array of M independent slits of width $2a$ and period Λ in a screen of thickness $b \ll \lambda$. The screen placed in vacuum is illuminated by a normally incident TM-polarized wave with wavelength $\lambda = 2\pi c/\omega = 2\pi/k$. The magnetic field of the wave $\vec{H}(x,y,z,t) = U(x)\exp(-i(kz+\omega t))\vec{e}_y$ is assumed to be time harmonic and constant in the y direction. The transmission of the slit array is determined by calculating all the light power $P(\lambda)$ radiated into the far-field diffraction zone, $x \in [-\infty, \infty]$ at the distance $z \gg \lambda$ from the screen. The total per-slit transmission coefficient, which represents the per-slit enhancement in transmission achieved by taking a single, isolated slit and placing it in an M-slit array, is then found by using an equation $T_M(\lambda) = P(\lambda)/MP_1$, where P_1 is the power radiated by a single slit. Figure 1 shows the transmission coefficient $T_M(\lambda)$, in the spectral region 500-2000 nm, calculated for the array parameters: a = 100 nm, Λ = 1800 nm, and $b = 5\times10^{-3}\lambda_{max}$. The transmitted power was computed by integrating the total energy flux at the distance z = 1 mm over the detector region of width Δx = 20 mm. The transmission spectra $T_M(\lambda)$ is shown for different values of M. We notice that the spectra $T_M(\lambda)$ is periodically modulated, as a function of wavelength, below and above a level defined by the transmission $T_1(\lambda) = 1$ of one isolated slit. As M is increased from 2 to 10, the visibility of the modulation fringes increases approximately from 0.2 to 0.7. The transmission T_M exhibits the Fabry-Perot like maxima around wavelengths $\lambda_n = \Lambda/n$ (n=1, 2, ...). The spectral peaks increase with increasing the number of slits and reach a saturation ($T_M^{max} \approx 5$) in amplitude by $M = 300$, at $\lambda \approx 1800$ nm. The peak widths and the spectral shifts of the resonances from the Fabry-Perot wavelengths decrease with increasing the number M of slits. From the data of Fig. 1, one can understand that enhancement and suppression in the transmission spectra are the natural properties of an ensemble of independent subwavelength slits in a thin ($b \ll \lambda$) screen. The spectral peaks are characterized by asymmetric Fano-like profiles. Such modulations in the transmission spectra are known as Wood's anomalies. The minima and maxima correspond to Rayleigh anomalies and Fano resonances, respectively [15]. A surprising prediction of the model is a weak Wood's anomaly, which is present in a classical Young type two-slit system ($M = 2$).

The above-presented data is based on rigorous calculation of the energy flux by using the electromagnetic field evaluated numerically. The transmission enhancement is achieved by taking a single, isolated slit and placing it in an array. The interference of the waves diffracted by independent slits can be considered as a physical mechanism responsible for the enhancement. To clarify the results of the computer code and gain physical insight into the enhancement mechanism, we have developed an analytical model, which yields simple formulae for the diffracted fields. For the fields diffracted by a narrow ($2a \ll \lambda, b \geq 0$) slit into the region $|z| > 2a$, it can be shown that the Neerhoff and Mur model simplifies to an analytical one. For the magnetic $\vec{H} = (0, H_y, 0)$ and electric $\vec{E} = (E_x, 0, E_z)$ fields we found:

$$H_y(x,z) = iaDF_0^1(k[x^2+z^2]^{1/2}), \quad (1)$$

$$E_x(x,z) = -az[x^2+z^2]^{-1/2}DF_1^1(k[x^2+z^2]^{1/2}), \quad (2)$$

and

$$E_z(x,z) = ax[x^2+z^2]^{-1/2}DF_1^1(k[x^2+z^2]^{1/2}), \quad (3)$$

where

$$D = 4k^{-1}[[\exp(ikb)(aA-k)]^2 - (aA+k)^2]^{-1} \quad (4)$$

and

$$A = F_0^1(ka) + \frac{\pi}{2}[\bar{F}_0(ka)F_1^1(ka) + \bar{F}_1(ka)F_0^1(ka)]. \quad (5)$$

Here, F_1^1, F_0^1, $\bar{F}_0$ and $\bar{F}_1$ are the Hankel and Struve functions, respectively. The fields are spatially nonuniform, in contrast to a common opinion that a subwavelength aperture diffracts light in all directions uniformly [16]. The fields produced by an array of M independent slits are given by $\vec{E}(x,z) = \sum_{m=1}^{M}\vec{E}_m(x+m\Lambda, z)$ and $\vec{H}(x,z) = \sum_{m=1}^{M}\vec{H}_m(x+m\Lambda, z)$, where $\vec{E}_m$ and $\vec{H}_m$ are the fields of an m-th beam generated by the respective slit. As an example, Fig. 2(a) compares the far-field distributions calculated by the analytical formulae (1-5) to

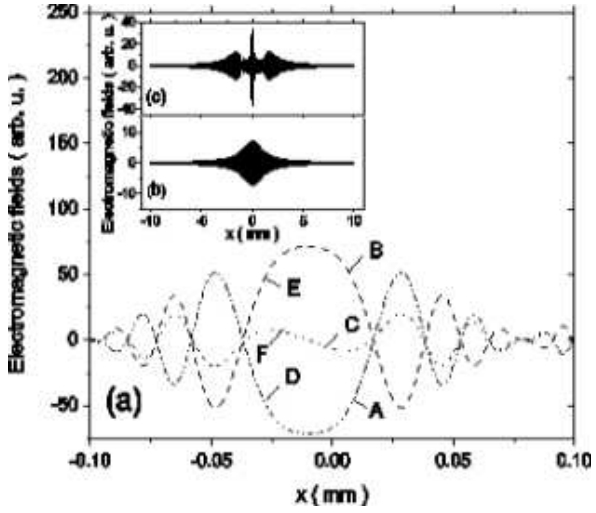

FIG. 2: Electromagnetic fields in the far-field zone. (a) The fields $\mathrm{Re}(E_x(x))$ (A and D), $\mathrm{Re}(H_y(x))$ (B and E), and $\mathrm{Re}(10E_z(x))$ (C and F) calculated for $M = 10$ and $\lambda = 1600$ nm. The curves A, B, and C: rigorous model; curves D, E, and F: analytical model. (b) $\mathrm{Re}(E_x(x))$ for M=1: analytical model. (c) $\mathrm{Re}(E_x(x))$ for M=5: analytical model.

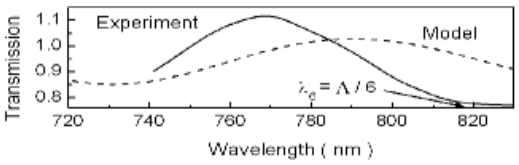

FIG. 3: The per-slit transmission coefficient $T(\lambda)$ versus wavelength for the Young type two-slit experiment [19]. Solid curve: experiment; dashed curve: analytical model. Parameters: $a = 100$ nm, $\Lambda = 4900$ nm, and $b = 210$ nm.

that obtained by the rigorous model. We notice that the distributions are undistinguishable. Thus, the analytical model not only supports results of our rigorous model, but presents an intuitively transparent explanation of the enhancement in terms of the interference of the beams produced by the multi-beam source. The array-induced decrease of the central beam divergence (Figs. 2(b) and 2(c)) is relevant to the beaming light [17], and the non-diffractive light and matter beams [18].

The analytical model accurately describes the fields $\vec{E}$ and $\vec{H}$, but what is about the transmission coefficient? The field power P, which determines the coefficient T_M, is found by integrating the energy flux $|\vec{S}| = |\vec{E} \times \vec{H}^* + \vec{E}^* \times \vec{H}|$. Thus, the model accurately explains also the light transmission. We now consider the predictions in light of the key observations published in the literature for the two fundamental systems of wave optics, the single-slit and two-slit systems. The major features of a single-slit system are the intraslit resonances and the spectral shifts of the resonances from the Fabry-Perot wavelengths [8]. In agreement with the predictions [8], the formula (4) shows that the transmission $T = P/P_0 = (a/k)[\mathrm{Re}(D)]^2 + [\mathrm{Im}(D)]^2$ exhibits Fabry-Perot like maxima around wavelengths $\lambda_n = 2b/n$, where P_0 is the power impinging on the slit opening. The enhancement and spectral shifts are explained by the wavelength dependent terms in the denominator of Eq. (4). The enhancement ($T(\lambda_1) \approx b/\pi a$ [18]) is in contrast to the attenuation predicted by the model [8]. The Young type two-slit configuration is characterized by a sinusoidal modulation of the transmission spectra $T_2(\lambda)$ [19, 20]. The modulation period is inversely proportional to the slit separation Λ. The visibility V of the fringes is of order 0.2, independently of the slit separation. In our model, the transmission is given by $T_2 \sim \int [F_1^1(x_1)[iF_0^1(x_1)]^* + F_1^1(x_2)^* iF_0^1(x_2)]dx$, where $x_1 = x$ and $x_2 = x + \Lambda$. The high-frequency modulations with the sideband-frequency $f_s(\Lambda) \approx f_1(\lambda) + f_2(\Lambda, \lambda) \sim 1/\Lambda$ (Figs. 1 and 3) are produced as in a classic heterodyne system by mixing two waves having different spatial frequencies, f_1 and f_2. Although our model ignores the plasmons, its prediction for the visibility ($V \approx 0.1$) of the fringes and the resonant wavelengths $\lambda_n = \Lambda/n$ compare well with the plasmon-assisted Young's type experiment [19] (Fig. 3). In the case of $b \geq \lambda/2$, the resonances at $\lambda_n = \Lambda/n$ can be accompanied by the intraslit resonances at $\lambda_n = 2b/n$. Some difference between the calculated and measured values shows that the plasmonless and plasmon-assisted resonances can compete in certain situations. It can be mentioned that although our model considers a screen of perfect conductivity, polarization charges develop on the metal surface. The proponents of surface polaritons, however, do not adhere strictly to traditional surface plasmons. We considered TM-polarized waves because TE modes are cutoff by a thick slit. In the case of a thin screen, TE modes propagate into slits so that magneto-polaritons develop. Because of the symmetry of Maxwell's equations the scattering intensity is formally identical with $\vec{E}$ and $\vec{H}$ swapping roles. Again, no traditional surface plasmons are present in our model.

In order to gain physical insight into the mechanism of plasmonless enhancement in a multi-slit ($M \geq 2$) system, we now consider the dependence of the transmission $T_M(\lambda)$ on the slit separation Λ. We assume that the slits are independent also at $\Lambda \to 0$. According to the Van Citter-Zernike coherence theorem, a light source (even incoherent) of radius $r = M(a + \Lambda)$ produces a transversally coherent wave at the distance $z \leq \pi R r/\lambda$ in the region of radius R. Thus, in the case of a subwavelength light source ($\Lambda \ll \lambda$), the collective emission of the ensemble of slits generates the coherent electric and magnetic fields, $\vec{E} = \sum_{m=1}^{M} \vec{E}_m \exp(i\varphi_m) \approx M\vec{E}_1 \exp(i\varphi)$ and $\vec{H} \approx M\vec{H}_1 \exp(i\varphi)$. This means that the beams arrive at the detector with the same phases $\varphi_m(x) \approx \varphi(x)$.

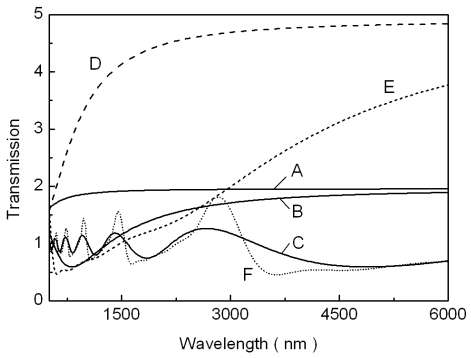

FIG. 4: The per-slit transmission $T_M(\lambda)$ versus wavelength for the different values of Λ and M: (A) $\Lambda = 100$ nm, $M = 2$; (B) $\Lambda = 500$ nm, $M = 2$; (C) $\Lambda = 3000$ nm, $M = 2$; (D) $\Lambda = 100$ nm, $M = 5$; (E) $\Lambda = 500$ nm, $M = 5$; (F) $\Lambda = 3000$ nm, $M = 5$. Parameters: $a = 100$ nm and $b = 10$ nm. There are two enhancement regimes at $\Lambda \ll \lambda$ and $\Lambda \geq \lambda$.

Consequently, the maximum power of the emitted light scales with the square of the number of slits (beams), $P \sim M^2$. Therefore, the transmission ($T_M \sim P/M$) grows linearly with the number of slits, $T_M \sim M$. For a given M, the function $T_M(\lambda)$ monotonically varies with λ. Such an enhancement regime (first regime) is shown in Fig. 4. At appropriate conditions, the transmission can reach 1000-times enhancement ($M = \lambda z/\pi R(a + \Lambda)$). The transmission enhancement in the second regime does not require close proximity of the slits. In the case of $R \geq \lambda z/\pi r$ ($\Lambda \geq \lambda$), the beams arrive at the detector with different phases φ_m. Consequently, the power and transmission grow slowly with the number of slits (Figs. 1-4). According to our model, the transmission T_M exhibits the Fabry-Perot like maxima around wavelengths $\lambda_n = \Lambda/n$. The constructive and destructive interference of the beams leads respectively to the enhancement and suppression of the transmission amplitudes as in a classical heterodyne system (Figs. 1 and 3).

The analytical model gives not only intuitively transparent explanation of the plasmonless transmission enhancement, but in contrast to the previous studies, predicts the enhancement for the matter waves. Indeed, in our model, the enhancement is based on coherent excitation of an assemble of slits and interference of the diffracted waves (beams). The constructive interference is provided not by coupling between the slits, but by a geometrically well-defined phase relationship between wave amplitudes produced by a subwavelength source at different lateral locations in the far field. Thus, the enhancement mechanism depends neither on the nature (light or matter) of the fields ψ_m nor on material and shape of the apertures. For instance, in the first enhancement regime, the fixed phase correlation leads to the M-times enhancement of the field amplitude, $\psi = \sum_{m=1}^{M} \psi_m \exp(i\varphi_m) \approx M\psi_1 \exp(i\varphi)$, and consequently to the M-time transmission enhancement. Due to Babinet's principle, the model predicts the enhancement also in the reflection spectra. Another surprising prediction of the model is a fact that the destructive interference of the fields at the detector can lead to the zero transmission. Indeed, the interference of the positive ($+\psi$) and *negative* ($-\psi = \psi \exp(i\varphi + \pi)$) fields produces a field with the zero amplitude and energy. Two subwavelength glass fibers of different length can be used to generate such fields. The value T=0 is obtained by summing up the respective positive and *negative* energies. Notice that the amplitudes of the fields ψ_m can rapidly decrease with increasing the distances x, y and z. However, due to the enhancement and beaming mechanisms (Figs. 1-4), an array produces a propagating wave ψ with low divergence. Such a behavior is in agreement with the Huygens-Fresnel principle, which considers a propagating wave as a superposition of secondary spherical waves.

The phenomena of enhanced and zero transmissions are strange and paradoxical from a point of view of the energy conservation. Indeed, the energy conservation is a general law of nature. In the classical physics, the energy W_{AB} of a conservative system AB that contains the objects A and B is equal to a sum of the positive energies W_A and W_B of the isolated objects A and B, $W_{AB} = W_A + W_B$. For an example, the kinetic energy K_{AB} of the system of two macroscopic objects is given by $K_{AB} = p_A^2/2m_A + p_B^2/2m_B$. If the objects A and B are two waves or they do have a wave nature of microscopic (quantum) objects, the energy conservation does not exhibit the law $W_{AB} = W_A + W_B$. It can be easily demonstrated that the energy of two harmonic light waves having the same amplitudes ($E_A = E_B = E_0$) and energies ($W_A = W_B = W_0 = E_0 E_0^* \int dx$) is given by $W_{AB} = W_A + W_B + 2E_0 E_0^* \int cos(\varphi_A(x) - \varphi_B(x))dx$, where $\varphi_A(x)$ and $\varphi_B(x)$ are the wave phases at the coordinate x, and $\Delta t = 1$. The interference term, which is the additional energy from a point of view of the classical (non-wave) physics, is the positive or *negative* energy associated with the wave phases. In the case of two waves having the same phases ($\varphi_A(x) = \varphi_B(x)$), the energy is given by $W_{AB} = W_0 + W_0 + 2W_0$, where $2W_0$ is the "*extra energy*" according to the classical physics. Correspondingly, the energy of the M waves is given by $W_M = M^2 W_0$. Another counter-intuitive feature of the two-wave system is the "*annihilation of energy*" ($W_{AB} = W_0 + W_0 + (-2W_0)$) in the case of $\varphi_A(x) - \varphi_B(x) = \pi$. Notice that the total energy is always positive, while the "additional" energy can be *negative*. The "*negative energy*" cannot be separated from the total positive energy of the system. Furthermore, the "*negative energy*" cannot be extracted from the system and transformed to the external system. Therefore, the "*negative energy*" can be considered as the internal virtual energy. Although, the construc-

tive and destructive interference are well known for the light intensity, up to now, the interference phenomenon for the energy has been considered as unphysical. We have showed the "non-classic energy conservation" based on the "*extra energy*", "*negative* energy" and "*annihilation of energy*" for multi-wave (multi-beam) systems in the context of extraordinary transmission of light and matter by subwavelength aperture arrays.

It is worth noting that the presented model is similar in spirit to the dynamical Bloch-waves diffraction model [21], the Airy-like model based on the Rayleigh field expansion [22], and especially to a diffracted evanescent wave model [11]. The difference arises from a fact that the models [11, 21, 22] consider the case of $M = \infty$, while predictions of our model strongly depend on the number $M \neq \infty$ of slits. In addition, our model deals with independent slits, while the models of Refs. [11, 21, 22] consider the slits electromagnetically coupled via the periodic boundary conditions. There is an evident resemblance also between our model and a Dicke superradiance model [23] of collective emission of an ensemble of atoms. A quantum reformulation of our model can help us to understand why a quantum entangled state of photons is preserved on passage through a hole array [24]. The quantum model will be presented in our next paper. Notice, that the surface waves can couple the radiation phases of the different slits, so that they get synchronized, and a collective emission can release the stored energy as an enhanced radiation. This kind of enhancement is of different nature compared to our model because the model does not require coupling between the slits.

In conclusion, we showed that the energy conservation does not exhibit the "classic law" if the physical objects are waves or they do have a wave nature of microscopic (quantum) objects. The "*extra energy*", "*negative* energy" and "*annihilation of energy*" are predicted for multi-wave (multi-beam) systems. The paradoxical phenomenon was demonstrated in context of the extraordinary transmission of light and matter through subwavelength aperture arrays assisted by surface waves [T.W. Ebbesen et al., Nature (London) 391, 667 (1998)) and E. Moreno et al., Phys. Rev. Lett. 95, 170406 (2005)]. The physical mechanism of "non-classic energy conservation" provides the transmission enhancement ("*extra energy*") not by coupling to the surface waves but by interference between diffracted waves (beams) in the far field. Furthermore, the "*annihilation of energy*" by destructive interference of fields at the detector leads to the zero transmission. Another surprising prediction of the model is a weak Wood's anomaly, which is present in a classical Young type two-slit system. The Wood anomalies in transmission spectra of optical gratings, a long standing problem in optics, follows naturally from interference properties of the model. We believe that the "non-classic energy conservation" demonstrated in the present paper gains physical inside into the nature of energy conservation. The physical mechanism of the "*extra energy*", "*negative* energy" and "*annihilation of energy*" affects the energy conservation in subwavelength systems. The mechanism can be used for numerous applications, for an example, in nanooptics and nanophotonics based on transmission and beaming of light or matter by subwavelengths apertures.

This study was supported by the Fifth Framework of the European Commission (Financial support from the EC for shared-cost RTD actions: research and technological development projects, demonstration projects and combined projects. Contract No NG6RD-CT-2001-00602) and in part by the Hungarian Scientific Research Foundation (OTKA, Contract Nos T046811 and M045644) and the Hungarian R&D Office (KPI, Contract No GVOP-3.2.1.-2004-04-0166/3.0).

[1] T.W. Ebbesen *et al.*, Nature (London) **391**, 667 (1998).
[2] W.L. Barnes *et al.*, Nature (London) **424**, 824 (2003).
[3] E. Moreno et al., Phys. Rev. Let. **95**, 170406 (2005).
[4] U. Schröter and D. Heitmann, Phys. Rev. B **58**, 15419 (1998).
[5] M.B. Sobnack, *et al.*, Phys. Rev. Lett. **80**, 5667 (1998).
[6] J.A. Porto, F.J. Garcia-Vidal, and J.B. Pendry, Phys. Rev. Lett. **83**, 2845 (1999).
[7] S. Astilean, P. Lalanne, and M. Palamaru, Opt. Comm. **175**, 265 (2000).
[8] Y. Takakura, Phys. Rev. Lett. **86**, 5601 (2001).
[9] P. Lalanne *et al.*, Phys. Rev. B **68**, 125404 (2003).
[10] A. Barbara *et al.*, Eur. Phys. J. D **23**, 143 (2003).
[11] H.J. Lezec and T. Thio, Opt. Exp. **12**, 3629 (2004).
[12] F. L. Neerhoff and G. Mur, Appl. Sci. Res. **28**, 73 (1973).
[13] R.F. Harrington and D.T. Auckland, IEEE Trans. Antennas Propag. **AP28**, 616 (1980).
[14] E. Betzig, A. Harootunian, A. Lewis, and M. Isaacson, Appl. Opt. **25**, 1890 (1986).
[15] A. Hessel and A.A. Oliner, Appl. Opt. **4**, 1275 (1965).
[16] H.J. Lezec *et al.*, Science **297**, 820 (2002).
[17] L. Martin-Moreno, F.J. Garcia-Vidal, H.J. Lezec, A. Degiron, T.W. Ebbesen, Phys. Rev. Lett. **90**, 167401 (2003).
[18] S.V. Kukhlevsky *et al.*, J. Mod. Opt. **50**, 2043 (2003), Opt. Commun. **231**, 35 (2004), Phys. Rev. B **70**, 195428 (2004).
[19] H.F. Schouten, *et al.*, Phys. Rev. Lett. **94**, 053901 (2005).
[20] P. Lalanne, *et al.*, Phys. Rev. Lett. **95**, 263902 (2005).
[21] M.M.J. Treacy, Appl. Phys. Lett. **75**, 606 (1999).
[22] Q. Cao and P. Lalanne, Phys. Rev. Lett. **88**, 057403 (2002).
[23] R.H. Dicke, Phys. Rev. Lett. **93**, 439 (1954).
[24] E. Altewischer, *et al.*, Nature (London) **418**, 304 (2002).